Neutrino Oscillations as an Open Quantum System

Author: Elisa Berto Guasp, ebertogu28@alumnes.ub.edu
Facultat de Física, Universitat de Barcelona, Diagonal 645, 08028 Barcelona, Spain.

Advisor: Jordi Salvadó Serra, jsalvado@ub.edu

Abstract: This work studies neutrino oscillations and how matter effects and environmental interactions influence neutrino detection. A semirealistic model of the Earth was implemented using four concentric layers of constant density based on the PREM profile, allowing simulation of atmospheric neutrino propagation with matter induced effects. Initial results in the standard three flavor framework justified neglecting the electron neutrino, motivating a simplified 2+1 model including muon, tau, and a hypothetical sterile neutrino. The impact of decoherence on neutrino evolution was then analyzed by incorporating dissipative terms into the Lindblad master equation. The results show a disappearance of muon neutrinos in specific regions of the oscillogram, driven by Earth matter effects at intermediate energies and stronger interferences at higher energies due to decoherence. These findings highlight how decoherence and sterile states could leave measurable imprints on future oscillation experiments.
Keywords: Neutrino oscillations, quantum superposition, non-standard interactions (NSI), sterile neutrino, decoherence.
SDGs: This TFG aligns with Sustainable Development Goal number 4 (Quality Education), as it contributes to high-level scientific education and the development of critical and technical skills in the field of particle physics.

I. INTRODUCTION

Neutrino oscillations stand as one of the most remarkable discoveries in contemporary particle physics, well established both theoretically and experimentally. Oscillations imply that neutrinos possess non-zero masses and that the weak-interaction eigenstates, commonly flavor basis, differ from the propagation eigenstates, mass basis.

In the neutrino-oscillation framework, the active flavor eigenstates ν_α ($\alpha = e, \mu, \tau$) are a coherent superposition of mass eigenstates ν_i ($i = 1, 2, 3$) and are related by the unitary Pontecorvo–Maki–Nakagawa–Sakata (PMNS) matrix $|\nu_\alpha\rangle = \sum_{i=1}^{3} U_{\alpha i} \, |\nu_i\rangle$ [1].

These mass eigenstates propagate through space with different phases due to their distinct masses. Coherence is maintained as neutrinos propagate through long distances which allows interference effects to produce flavor transitions.

Real neutrinos rarely evolve in perfect isolation from their environment, and will, in general, become entangled with a large number of environmental degrees of freedom. As a result, these interactions induce non-unitary effects in their propagation, leading to a loss of quantum coherence. This suppression of interference phenomena is known as decoherence, and it can be consistently incorporated into the theoretical framework using the Lindblad master equation. There will not be any further discussion of the microscopic origin of such decoherence effects, instead the approach will remain purely phenomenological, focusing on how these non-unitary effects alter neutrino evolution within the open quantum system approach.

Following this phenomenological perspective, decoherence manifests in oscillation experiments as a damping of the usual interference terms. The most common parametrization of decoherence rates is $\Gamma_{ij}(E) = \Gamma_{ij}(E_0)\left(\frac{E}{E_0}\right)^n$ with $n = 0, \pm 1, \pm 2$. In particular $n = 1$ will be used since these sterile neutrino simulations focus on high energies and this choice is most appropriate for future comparison with IceCube data and computing efficiency. The analysis in Ref. [2] applied this model to eight years of IceCube/DeepCore atmospheric neutrino data, leading to upper limits on the coefficients γ_{ij}. Specifically, for $n = 1$ the bounds are $\gamma_{21} \lesssim 10^{-24}\,\text{GeV}$ and $\gamma_{31}, \gamma_{32} \lesssim 10^{-24}\,\text{GeV}$, whereas for $n = 2$ the limits weaken to approximately $\mathcal{O}(10^{-26}\,\text{GeV})$. These constraints provide a benchmark region that these simulations will explore when combining decoherence with a sterile-neutrino state. As for the sterile neutrino parameters, the IceCube collaboration in Ref. [3] analysed 10.5 years of data and provides the best fitting points for the mixing angle and the square mass difference at $\sin^2 2\theta = 0.16$ and $\Delta m_{41} = 3.5\text{eV}^2$.

II. FORMALISM

A. Neutrino oscillations in vacuum and matter

In quantum mechanics, the time evolution of a mixed state is governed by the von Neumann equation,

$$\frac{d}{dt}\rho(t) = -i[\mathcal{H}, \rho(t)]. \tag{1}$$

Here $\rho(t)$ is the density matrix of the system and $\mathcal{H}$

is the Hermitian Hamiltonian operator responsible for the unitary component of the dynamics. In the effective mass basis, standard neutrino oscillations in vacuum are described by

$$\mathcal{H} = \frac{1}{2E}\begin{pmatrix} 0 & 0 & 0 \\ 0 & \Delta m^2_{21} & 0 \\ 0 & 0 & \Delta m^2_{31} \end{pmatrix}, \tag{2}$$

where E is the energy of the neutrino and Δm^2_{ij} is the squared mass difference. Since normal ordering is used $\Delta m^2_{21} = 7.49 \times 10^{-5}\text{eV}^2$ and $\Delta m^2_{31} = 2.534 \times 10^{-3}\text{eV}^2$.

When neutrinos travel through a background of particles, they undergo coherent forward scattering with the surrounding matter. These interactions lead to modifications of the properties of neutrinos as well as the oscillations behaviour. This is known as the matter effect, and has played a key role in interpreting various neutrino oscillation data. In the standard three neutrino framework, the effective Hamiltonian $\tilde{\mathcal{H}}$ in the mass basis, which governs neutrino propagation in the presence of matter, differs from the Hamiltonian in vacuum as

$$\tilde{\mathcal{H}} = \mathcal{H} + \mathcal{H}', \tag{3}$$

where $\mathcal{H}$ is the Hamiltonian in Eq.(2) and $\mathcal{H}'$ is:

$$\mathcal{H}' = U^\dagger \begin{pmatrix} V_{CC} + V_{NC} & 0 & 0 \\ 0 & V_{NC} & 0 \\ 0 & 0 & V_{NC} \end{pmatrix} U. \tag{4}$$

V_{CC} and V_{NC} are the charged and neutral current matter potentials respectively, which are functions of the electron an neutron density, N_e and N_n,

$$V_{CC} = \sqrt{2} G_F N_e \qquad V_{NC} = -\frac{1}{\sqrt{2}} G_F N_n, \tag{5}$$

where G_F is the Fermi constants. For this work only the charged current potential will be taken into account since neutral current is a diagonal term that develops just a common phase for all three flavors, and does not affect the neutrino oscillation behaviours.

All simulations involving this framework assume normal mass ordering for the squared mass differences and the mixing matrix angles. The values used are from Ref. [1].

B. Decoherence

Decoherence describes the process by which neutrino mass eigenstates lose their quantum coherence as the system becomes entangled with its surrounding environment. For dissipative systems is common to describe the time evolution of the density matrix, $\rho(t)$, using the Lindblad Master equation [4],

$$\frac{d\rho}{dt} = -i\,[\mathcal{H},\,\rho] \;+\; \sum_k^{N^2-1} \Big(L_k\,\rho\,L_k^\dagger \;-\; \tfrac{1}{2}\{L_k^\dagger L_k, \rho\}\Big). \tag{6}$$

The first term is simply the von Neumann equation for unitary evolution of a closed quantum system where $\mathcal{H}$ is the system's Hamiltonian.

The second term represents the dissipative contribution to the evolution and must satisfy certain conditions to ensure total probability is conserved. In particular, the evolution must be completely positive and trace preserving. The energy conservation of the subsystem is also required. This condition implies disregarding certain types of decoherence effects that would damp non-oscillatory terms in oscillation probabilities, such relaxation effects cause loss of information about the initial state.

Here the set of jump operators L_k provides a controlled, phenomenological way to introduce decoherence or dissipation, whether sourced by stochastic density fluctuations, quantum gravity effects, etc. Without abandoning the framework of quantum mechanics. These are $N \times N$ complex matrices with N the dimension of the Hilbert space of the subsystem.

While working with three active neutrinos the elements of the Lindblad equation can be expanded using the $SU(3)$ generators, the Gell-Mann matrices λ_i, as a basis. In Einstein's notation: $H = H_i\lambda_i,\ \rho = \rho_j\lambda_j$. And so Eq.(6) reads as

$$\frac{d}{dt}\rho_k(t)\lambda_k = f^{ijk}H_i\rho_j(t)\lambda_k + D_{kl}\rho_l\lambda_k. \tag{7}$$

f^{ijk} are structure constants completely antisymmetric and D_{kl} is a symmetric and trace preserving matrix that encodes all decoherence effects. Under the conditions previously stated the dissipative matrix takes the form:

$$D_{kl} = -\mathrm{Diag}\{\Gamma_{21}, \Gamma_{21}, 0, \Gamma_{31}, \Gamma_{31}, \Gamma_{32}, \Gamma_{32}, 0\}. \tag{8}$$

The elements of the dissipative matrix trace are the decoherence parameters and act as damping rates for the interference terms in the oscillation probabilities. The focus of this study is not on the origin of such entanglement but how these dumping terms affect neutrino oscillations. After solving the Lindblad equation and some algebra, one finds:

$$\begin{aligned} P_{\nu_\alpha\nu_{\alpha'}} = \delta_{\alpha\alpha'} &- 2\sum_{j>k}\mathrm{Re}(\tilde{U}_{\alpha' j}\tilde{U}^*_{\alpha j}\tilde{U}_{\alpha k}\tilde{U}^*_{\alpha' k}) \\ &+ 2\sum_{j>k}\mathrm{Re}(\tilde{U}_{\alpha' j}\tilde{U}^*_{\alpha j}\tilde{U}_{\alpha k}\tilde{U}^*_{\alpha' k})\, e^{-\Gamma_{jk}x}\cos\left(\frac{\tilde{\Delta}_{jk}}{2E}x\right) \\ &+ 2\sum_{j>k}\mathrm{Im}(\tilde{U}_{\alpha' j}\tilde{U}^*_{\alpha j}\tilde{U}_{\alpha k}\tilde{U}^*_{\alpha' k})\, e^{-\Gamma_{jk}x}\sin\left(\frac{\tilde{\Delta}_{jk}}{2E}x\right) \end{aligned} \tag{9}$$

FIG.1 shows how this decoherence parameters affect to the $\nu_\mu \to \nu_\mu$ probability depending on the energy.

C. Sterile neutrino

Sterile neutrinos are hypothetical gauge-singlet states that do not participate in Standard Model weak interactions, and whose existence remains unconfirmed. If they

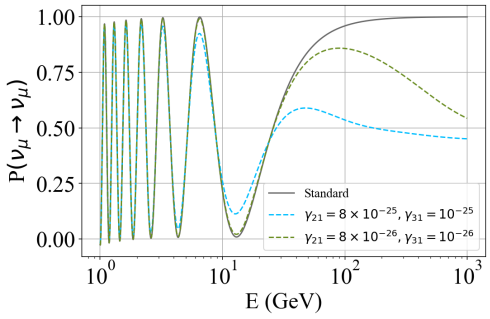

FIG. 1: Oscillation probability of a muon neutrino in vacuum. Solid line is standard oscillation, blue and green dashed line are deviations due to the decoherence parameters in the legend. The dependency on energy is n=1.

mix with the standard three flavor neutrinos, they introduce an additional oscillation scale $\Delta m^2_{41} \sim \mathcal{O}(1\text{eV}^2)$, far larger than solar or atmospheric scales.

In this work, instead of opting for a 3+1 model to incorporate the sterile neutrino into the neutrino oscillation framework, a 2+1 model will be adopted, based on simulations carried in section III, where the electron flavor is omitted, thereby simplifying the simulations. The mixing angles used for the simulations are:

TABLE I: Mixing angles for the PMNS matrix used. θ_{42} and θ_{43} take the place of θ_{12} and θ_{13} respectively.

$\sin^2\theta_{42}$	$\sin^2\theta_{23}$	$\sin^2\theta_{43}$
0.16	0.56	0.00

Decoherence with sterile neutrinos is a lot less bounded than standard neutrinos and allows for a larger margin to investigate new physics and produce predictions that could guide future experiments. Since sterile neutrinos have yet to be confirmed, there is no reason to rule out decoherence effects a priori.

III. ATMOSPHERIC NEUTRINOS

Atmospheric neutrino detectors , like Super-Kamiokandem, IceCube or ANTARES, have the highest sensitivity and statistics for muon neutrinos. These produce long, track like events that are easier to detect and reconstruct than electron or tau events. Hence, focusing mainly on muonic neutrino oscillations allows to directly compare theoretical predictions to the existing data.

When accounting for matter effects in the study of atmospheric neutrinos, it becomes essential to consider the Earth's density profile. For this work the PREM model [5] is taken as a reference. The Earth's interior is modelled as consisting of four concentric layers, each with constant matter density. To estimate the electron density of each layer, a weighted average of the electron number per atom was computed based on the elemental composition of the corresponding region.

Using simple algebra it is easy to parametrize any trajectory using the zenith angle and since only neutrinos that have gone through earth are on interest only the under half of zenith angle is used. With PREM data one separate the calculus into four different sections where neutrinos go through one, two, three or four different layers. Once the Earth's matter profile is parametrized, a first simulation is carried out within the standard three flavour framework, FIG.2 show for a constant trajectory the oscillation probabilities for an initial muon neutrino as a function of energy. The results provide a consistent basis for adopting a simplified 2+1 model including sterile, muon, and tau neutrinos since electric neutrino contribution is notoriously smaller.

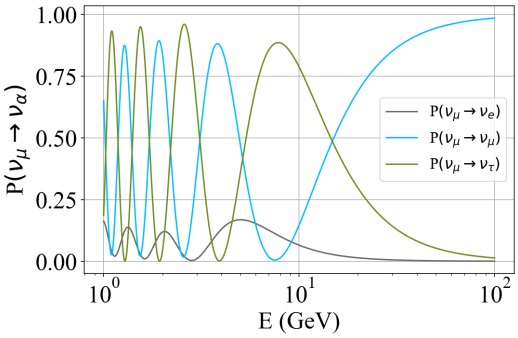

FIG. 2: Muon neutrino oscillation probability to be detected as muon (blue line), electron(grey line) or tau(green line) in function of energy for a constant trajectory (Zenith angle = 104.5°). It shows electron neutrino amplitude has the smallest contribution.

This simplification reduces computational complexity while still capturing the key features of muon neutrino oscillations in matter.

The following oscillograms show the behaviour of neutrinos and antineutrinos probabilities through all earth layers for different energies. Energy range is the order of TeV due to the oscillation scale of sterile neutrinos being orders of magnitude larger than standard neutrinos.

Observing the antineutrino oscillogram, FIG.3, there is a notorious muon disappearance between $10^3 - 10^4$GeV in the trajectories closest to the Earth's core. This effect is due to a matter enhanced resonance between the matter potential and Δm^2_{41} that boosts muon to sterile conversion. However, due to the chosen mixing angles (TABLE I), part of the disappearing muon antineutrinos also oscillate into tau antineutrinos. As for FIG.4, a similar effect is observed but at lower energies due to the opposite sign of the matter potential.

IV. DECOHERENCE EFFECT IN STERILE ATMOSPHERIC NEUTRINO SEARCHES

To incorporate decoherence into the previous results it's necessary to solve Eq.(6) introducing both, the sterile neutrino framework and matter effects with Earth matter

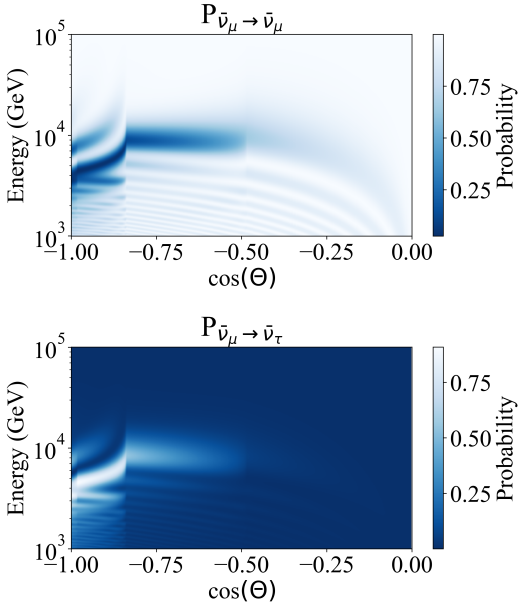

FIG. 3: Oscillograms for the muon antineutrino probabilities assuming normal mass ordering. Only matter interactions are accounted for.

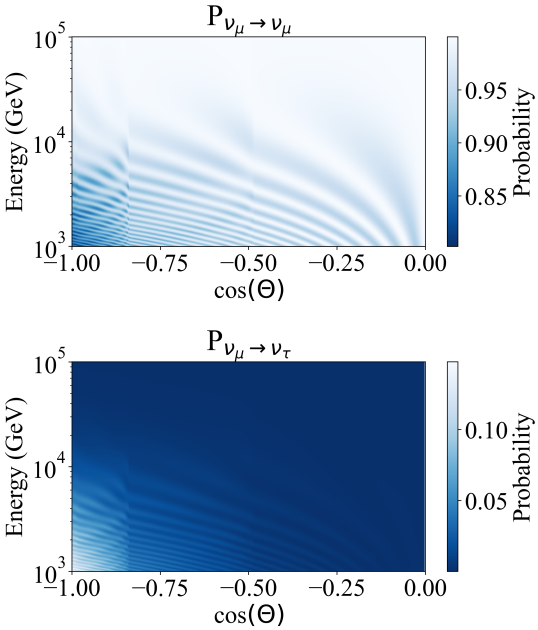

FIG. 4: Oscillograms for the muon neutrino probabilities assuming normal mass ordering. Only matter interactions are accounted for.

profile. To obtain a numerical solution for the evolution of the neutrino density matrix, the `solve_ivp` function from the `scipy.integrate` module was employed [6, 7]. The main benefits from using this function are the control over tolerance and precision, and the adaptive time stepping. It uses adaptive step size control that ensures high numerical accuracy without wasting time on unnecessarily small steps when not needed.

The results in FIG.5 and FIG.6 show a disappearance of muon neutrinos and antineutrinos at high energies due to the decoherence parameters dependency on energy being lineal for n= 1, which is the dependency explored in this work.

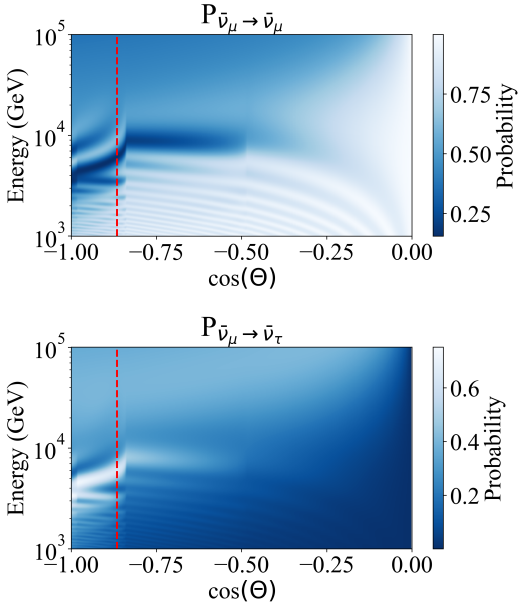

FIG. 5: Oscillograms for the muon antineutrino probabilities assuming normal mass ordering. Decoherence parameters are $\gamma_{32} = \gamma_{31} = \gamma_{21} = 10^{-27}$ GeV, with an exponential dependency on energy of n = 1. The red line marks 150°, constant angle represented at FIG. 7.

This dumping effect is more noticeable in FIG. 7. In the first range of energies, closer to 1 TeV, decoherence effects are hard to notice especially for $\gamma_{ij} = 10^{-28}$. However when getting closer to 100 TeV there is a considerable difference between the predictions with and without decoherence.

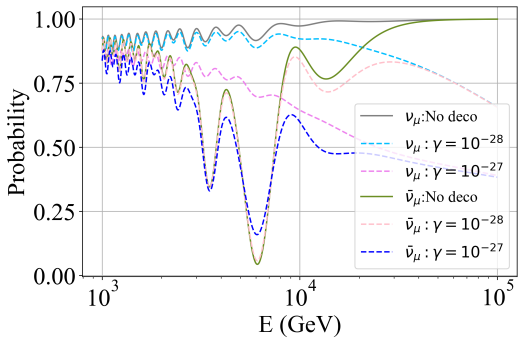

FIG. 7: Section of the colormap with constant angle 150°. Plots the probabilities for muon neutrinos and antineutrinos with and without decoherence. Two different decoherence parameters values are represented, showing larger dumping effects for larger values.

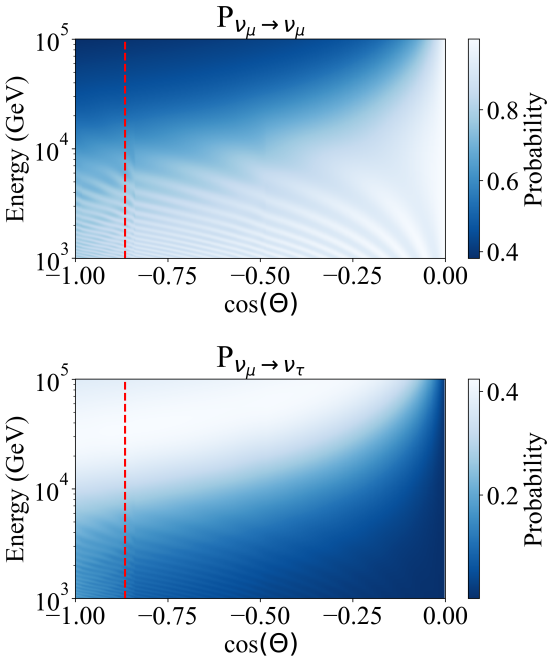

FIG. 6: Oscillograms for the muon neutrino probabilities assuming normal mass ordering. Decoherence parameters are $\gamma_{32} = \gamma_{31} = \gamma_{21} = 10^{-27}$ GeV. The red line marks 150°, constant angle represented at FIG. 7.

V. CONCLUSIONS

This study has explored the impact of matter effects and decoherence on muon neutrino oscillations in a 2+1 flavour framework including a sterile neutrino. The simulation of atmospheric neutrinos propagating through a semirealistic Earth model showed a significant muon disappearance in trajectories crossing the core, particularly around 1–10 TeV for antineutrinos, due to a matter-enhanced resonance with the sterile state. When including decoherence, an additional high energy suppression on ν_μ survival probabilities appears, further reducing the expected muon neutrino flux at the detector with the exception of the antineutrino disappearance near 10 TeV where decoherence appears to increase detection probabilities.

These results suggest that decoherence could play a non negligible role in oscillation experiments like IceCube. In particular, it may reduce the experiment's sensitivity to the disappearances induced by the sterile neutrino. This would weaken IceCube's ability to exclude sterile neutrinos, potentially reconciling its null results with other experiments that do observe hints of sterile states.

These simulations involve several approximations, such as modeling the Earth with four constant density layers, reducing the flavour space to a 2+1 framework, and assuming equal decoherence rates. Nonetheless, the results capture the key physical effects and offer qualitative insight into how matter and decoherence could impact atmospheric neutrino observations in large scale experiments. The next step would be to analyse actual atmospheric neutrino data, using the calculations developed in this work as inputs for the interpretation.

Acknowledgments

I want to thank my advisor Jordi Salvador for helping me with the project and being there anytime I needed advise. I want to also thank my friends and family for supporting me during this tough process, and in particular Pau, for taking the time of reading this memory several times and giving me feedback.

[1] Ivan Esteban, M. C. Gonzalez-Garcia, Michele Maltoni, Ivan Martinez-Soler, João Paulo Pinheiro, and Thomas Schwetz. NuFit-6.0: updated global analysis of three-flavor neutrino oscillations. *JHEP*, 12:216, 2024.

[2] Pilar Coloma, Jacobo Lopez-Pavon, Ivan Martinez-Soler, and Hiroshi Nunokawa. Decoherence in Neutrino Propagation Through Matter, and Bounds from IceCube/DeepCore. *Eur. Phys. J. C*, 78(8):614, 2018.

[3] R. Abbasi et al. Methods and stability tests associated with the sterile neutrino search using improved high-energy $\nu\mu$ event reconstruction in IceCube. *Phys. Rev. D*, 110(9):092009, 2024.

[4] Goran Lindblad. On the Generators of Quantum Dynamical Semigroups. *Commun. Math. Phys.*, 48:119, 1976.

[5] A. M. Dziewonski and D. L. Anderson. Preliminary reference earth model. *Physics of the Earth and Planetary Interiors*, 25(4):297–356, 1981.

[6] Pauli Virtanen, Ralf Gommers, Travis E. Oliphant, and et al. Scipy 1.0: Fundamental algorithms for scientific computing in python. *Nature Methods*, 17:261–272, 2020.

[7] SciPy Community. scipy.integrate.solve_ivp. https://docs.scipy.org/doc/scipy/reference/generated/scipy.integrate.solve_ivp.html, 2024.

Preparació del manuscript del TFG amb LaTeX

Author: Elisa Berto Guasp, ebertogu28@alumnes.ub.edu
Facultat de Física, Universitat de Barcelona, Diagonal 645, 08028 Barcelona, Spain.

Advisor: Jordi Salvadó Serra, jsalvado@ub.edu

Resum: En aquest treball s'estudien les oscil·lacions de neutrins i com els efectes de la matèria i les interaccions amb l'ambient influeixen en les deteccions de neutrins. S'ha implementat un model semirealista de la Terra amb quatre capes concèntriques de densitat constant basades en el perfil PREM. Aquest model permet realitzar simulacions atmosfèriques de la propagació dels neutrins i els efectes induïts per la interacció amb la matèria. Els primers resultats de les simulacions justifiquen la negligència dels neutrins electrònics, motivant un model simplificat 2+1 que inclou els neutrins muó, tau i l'hipotètic estèril. L'impacte de la decoherència sobre l'evolució dels neutrins s'ha analitzat incorporant termes dissipatius amb l'equació de Lindblad mestra. Els resultats mostren una desaparició dels neutrins en regions específiques de l'oscil·lograma, deguda als efectes de la matèria de la Terra a energies intermèdies i interferències més fortes a altes energies a causa de la decoherència. Aquests resultats suggereixen que la decoherència amb la hipòtesi d'un neutrí estèril podria tenir efectes observables en futurs experiments d'oscil·lacions.
Paraules clau: Oscil·lacions de neutrins, superposició quàntica, interaccions no estàndars, decoherència, nuetrí estèril.
ODSs: Aquest TFG s'alinea amb l'Objectiu de Desenvolupament Sostenible número 4 (Educació de qualitat), ja que contribueix a la formació científica d'alt nivell i al desenvolupament de competències crítiques i tècniques en l'àmbit de la física de partícules.

Objectius de Desenvolupament Sostenible (ODSs o SDGs)

1. Fi de la es desigualtats		10. Reducció de les desigualtats	
2. Fam zero		11. Ciutats i comunitats sostenibles	
3. Salut i benestar		12. Consum i producció responsables	
4. Educació de qualitat	X	13. Acció climàtica	
5. Igualtat de gènere		14. Vida submarina	
6. Aigua neta i sanejament		15. Vida terrestre	
7. Energia neta i sostenible		16. Pau, justícia i institucions sòlides	
8. Treball digne i creixement econòmic		17. Aliança pels objectius	
9. Indústria, innovació, infraestructures			

Appendix A: MUON TO STERILE NEUTRINO OSCILLOGRAMS

With current sterile neutrinos hypotheses, these are not directly detectable with existing experiments since they don't interact under Standard Model forces. However, the simulations in this work allow for a prediction of their appearance probability.

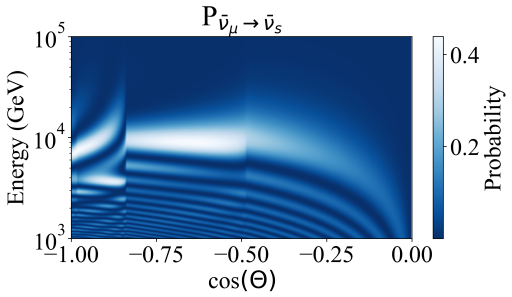

FIG. 8: Oscillogram for appearance probabilities of sterile antineutrinos. Only matter interactions are accounted for.

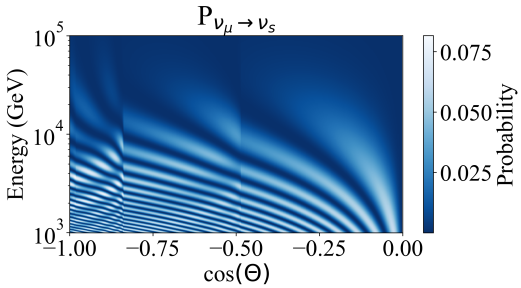

FIG. 9: Oscillogram for appearance probabilities of sterile neutrinos. Only matter interactions are accounted for.

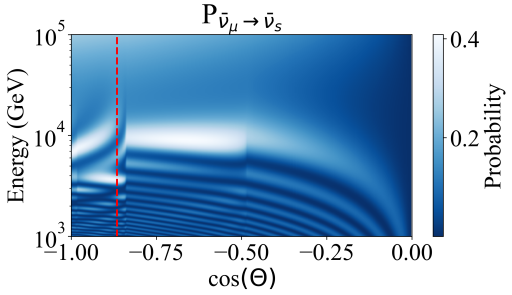

FIG. 10: Oscillogram for appearance probabilities of sterile antineutrinos considering matter interactions and decoherence. Decoherence parameters are $\gamma_{32} = \gamma_{31} = \gamma_{21} = 10^{-27}$ GeV. The red line marks 150°, constant angle represented at FIG. 7.

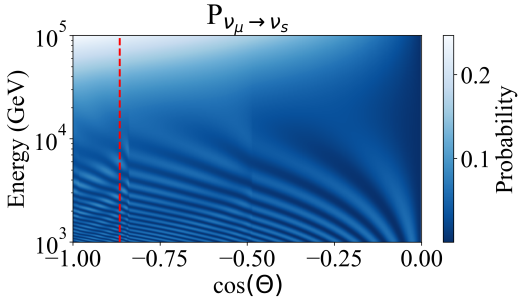

FIG. 11: Oscillogram for appearance probabilities of sterile neutrinos considering matter interactions and decoherence. Decoherence parameters are $\gamma_{32} = \gamma_{31} = \gamma_{21} = 10^{-27}$ GeV. The red line marks 150°, constant angle represented at FIG. 7.